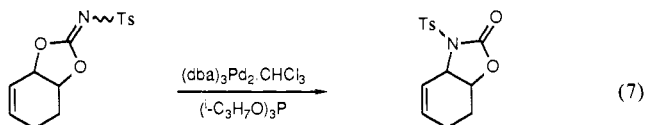


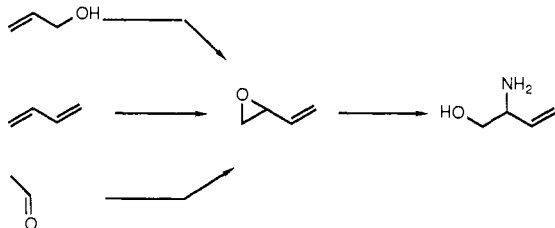
CH<sub>3</sub>OH)], as outlined in Scheme I. The key conversion of the enantiomerically pure vinyl epoxide 7 to the 2-oxazolidone proceeds with complete retention of configuration.

This metal-catalyzed facile (0 °C to room temperature) opening of vinyl epoxides with retention of configuration makes amino alcohol derivatives of defined stereochemistry readily available. The reaction course most simply may be interpreted in terms of path c of eq 1; however, the question of O vs. N alkylation in a kinetic sense is not established. We have determined that products of O-alkylation do rearrange to the products of N-cyclization in the presence of the Pd(0) catalyst (eq 7). Thus, it is possible



that the kinetic products of cyclization in the Pd(0) opening of vinyl epoxides with isocyanates are the imino carbonates which subsequently rearrange to the presumed thermodynamically more stable 2-oxazolidones. Further work on the mechanism and scope of the reaction is in progress.

Synthetically, the availability of vinyl epoxides from olefins makes this sequence the equivalent of hydroxyamination of an olefin. Alternatively, the availability of the vinyl epoxides via



a sulfur ylide addition<sup>19</sup> to carbonyl partners makes this sequence equivalent to a regiocontrolled addition of an allylamine anion to a carbonyl group.

**Acknowledgment.** We thank the National Science Foundation and the National Institutes of Health, General Medical Sciences, for their generous support of our programs.

(17) For catalytic epoxidation conditions, see: Hanson, R. M.; Sharpless, K. B. *J. Org. Chem.* **1986**, *51*, 1922. Epoxidation with MCPBA gives a 1:1.8 mixture of the desired epoxide and its diastereomer. For an alternative approach for diastereoselective epoxidation, see: Hasan, I.; Kishi, Y. *Tetrahedron Lett.* **1980**, *21*, 4229.

(18) For oxidation conditions, see: Herscovici, J.; Antonakis, K. *J. Chem. Soc., Chem. Commun.* **1980**, 561.

(19) Rosenberger, M.; Newkom, C.; Aig, E. R. *J. Am. Chem. Soc.* **1983**, *105*, 3656.

## Return Electron Transfer within Geminate Radical Ion Pairs. Observation of the Marcus Inverted Region

Ian R. Gould,\* Deniz Ege, Susan L. Mattes, and Samir Farid\*

Corporate Research Laboratories, Eastman Kodak Company  
Rochester, New York 14650

Received December 30, 1986

In recent years the physical and chemical properties of photoinduced electron-transfer reactions have been extensively studied,<sup>1</sup> with particular emphasis on maximizing the efficiency of charge separation.<sup>2</sup> However, energy-wasting return electron transfer, especially within the primary geminate radical ion pair for singlet-state reactions, often results in low quantum yields for free-ion formation.<sup>1,2</sup> Detailed studies of the mechanisms and kinetics of product formation for several photosensitized electron-transfer reactions suggest that a relationship exists between the thermodynamics and the kinetics of the return electron transfer process.<sup>1a,3</sup> In this work we summarize the results of laser flash photolysis studies which were specifically designed to study this relationship. The results provide a clear example of the Marcus "inverted region" in these processes.<sup>4</sup>

Experiments were performed in degassed acetonitrile at room temperature using 9,10-dicyanoanthracene (DCA) and 2,6,9,10-tetracyanoanthracene (TCA) as the excited-state sensitizers and electron acceptors and naphthalene derivatives, diphenylacetylene, and biphenyl as the electron donors (Table I). Absolute quantum yields for formation of free radical ions ( $\Phi_{\text{sep}}$ ) were determined by using conventional laser flash photolysis. In each case, the excited acceptor was efficiently quenched by the electron donors; otherwise, minor corrections for incomplete interception were made. 4,4'-Dimethoxystilbene (DMS,  $5 \times 10^{-4}$  M) was added to scavenge the radical cations which escaped the radical ion pair. The low concentration of DMS ensured that interception of the excited acceptor or of the geminate pair by DMS was insignificant. The same transient species, the DMS radical cation, was monitored irrespective of the donor/acceptor pair. The relative amounts of DMS radical cation observed for the different donor/acceptor pairs gave the relative quantum yields for free-ion formation ( $\Phi_{\text{sep}}$ ) directly (Table I). The relative yields were converted to absolute yields by using the benzophenone triplet state as an actinometer.<sup>5a,b,6</sup>

A highly simplified mechanism which, however, includes the important processes required to understand the data is shown in Scheme I. Electron transfer from the donors to the excited-state acceptors is exothermic, and so other quenching mechanisms are not expected to be important. Weak exciplex emission can be detected for several of the donor/acceptor pairs, but the only process of significance for these exciplexes is geminate ion pair formation.<sup>5d,e</sup>

(1) (a) Mattes, S. L.; Farid, S. In *Organic Photochemistry*; Padwa, A., Ed.; Marcel Dekker: New York, 1983; Vol. 6, p 233. (b) Davidson, R. S. In *Advances in Physical Organic Chemistry*; Gold, V., Bethell, D., Eds.; Academic: London, 1983; Vol. 19, p 130. (c) Mattes, S. L.; Farid, S. *Science (Washington, DC)* **1984**, *226*, 917. (d) Kavarnos, G. J.; Turro, N. J. *Chem. Rev.* **1986**, *86*, 401.

(2) See, for example: Fox, M. A. In *Advances in Photochemistry*; Volman, D. H., Gollnick, K., Hammond, G. S., Eds.; Wiley: New York, 1986; Vol. 13, p 237.

(3) (a) Mattes, S. L.; Farid, S. *J. Chem. Soc., Chem. Commun.* **1980**, 126. (b) Mattes, S. L.; Farid, S. *J. Am. Chem. Soc.* **1983**, *105*, 1386. (c) Mattes, S. L.; Farid, S. *J. Am. Chem. Soc.* **1986**, *108*, 7356.

(4) (a) Marcus, R. A. *J. Chem. Phys.* **1956**, *24*, 966. (b) Marcus, R. A. *Annu. Rev. Phys. Chem.* **1964**, *15*, 155.

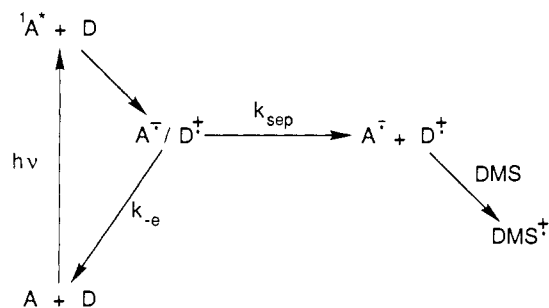
(5) (a) Details of these experiments will be reported in a full publication. (b) A similar value of  $\Phi_{\text{sep}}$  for the dicyanoanthracene/diphenylacetylene pair is obtained from steady-state product analysis experiments in which diphenylacetylene is used as a cosensitizer for the decomposition of benzyltrimethylsilane (ref 5c). (c) Mattes, S.; Farid, S., unpublished results. (d) Gould, I. R.; Kennedy, T. J.; Farid, S., unpublished results. (e) Weller, A. Z. *Phys. Chem. (Wiesbaden)* **1982**, *130*, 129.

(6) The values of  $\Phi_{\text{sep}}$  were observed to be concentration dependent (ref 5a). The data in Table I are extrapolated to zero concentration.

**Table I.** Absolute Quantum Yields for Separated Ion Formation for Quenching of Cyanoanthracene Excited Singlet States by Various Hydrocarbon Donors

donor	acceptor	$\Phi_{\text{sep}}$	$k_{-e}$ , s <sup>-1</sup>	$E_{\text{ox}}$ , V <sup>a</sup>	$-\Delta G_{-e}$ , eV
biphenyl	DCA	~0.83 <sup>b</sup>	~1.0 × 10 <sup>8</sup>	1.52	2.90
diphenylacetylene	DCA	0.760	1.58 × 10 <sup>8</sup>	1.41	2.79
naphthalene	DCA	0.571	3.76 × 10 <sup>8</sup>	1.36	2.74
2-methyl-naphthalene	DCA	0.425	6.76 × 10 <sup>8</sup>	1.24	2.62
2,6-dimethyl-naphthalene	DCA	0.340	9.70 × 10 <sup>8</sup>	1.15	2.53
biphenyl	TCA	0.246	1.53 × 10 <sup>9</sup>	1.52	2.40
diphenylacetylene	TCA	0.201	1.99 × 10 <sup>9</sup>	1.41	2.29
naphthalene	TCA	0.125	3.50 × 10 <sup>9</sup>	1.36	2.24
2-methyl-naphthalene	TCA	0.099	4.55 × 10 <sup>9</sup>	1.24	2.12
2,6-dimethyl-naphthalene	TCA	0.068	6.85 × 10 <sup>9</sup>	1.15	2.03

<sup>a</sup>Oxidation potentials vs. ferrocene in methylene chloride with 2% trifluoroacetic acid and 2% trifluoroacetic anhydride at a frequency of 5000 Hz with a 50-mV square-wave amplitude and a 5-mV step height (ref 5a, 8). Under the same conditions the oxidation potential of DMS is 0.61 and the reduction potentials of DCA and TCA are -1.38 and -0.88 V vs. ferrocene. The peaks of the reverse waves for biphenyl and naphthalene were not clearly defined. <sup>b</sup>The measured  $\Phi_{\text{sep}}$  is 0.75. However, in this case geminate pair formation is almost isoenergetic, and we estimate that ion pairs are formed at only ca. 90% efficiency.

**Scheme I**

From steady-state product analysis studies the rate of diffusive separation ( $k_{\text{sep}}$ ) for two reactions of the acceptors used in the present work has been determined to be ca.  $5 \times 10^8 \text{ s}^{-1}$ .<sup>3</sup> Independently, Weller et al. determined the same value for this rate, for the pyrene/dimethylaniline radical ion pair in acetonitrile at room temperature.<sup>7</sup> It is thus a reasonable assumption that variations in  $k_{\text{sep}}$  are not responsible for the variations in  $\Phi_{\text{sep}}$ , at least for the radical ion pairs studied in the present work, which were designed to have very similar structures. The values of  $\Phi_{\text{sep}}$  are given by eq 1,  $k_{-e}$  can be evaluated by taking  $k_{\text{sep}}$  as a constant

$$\Phi_{\text{sep}} = k_{\text{sep}} / (k_{\text{sep}} + k_{-e}) \quad (1)$$

$$\Delta G_{-e} = E_{\text{red}}(\text{A}) - E_{\text{ox}}(\text{D}) \quad (2)$$

value of  $5 \times 10^8 \text{ s}^{-1}$  (Table I). The free energy changes for each of the electron-transfer reactions,  $k_{-e}$  ( $\Delta G_{-e}$ ), were obtained from the oxidation potentials of the donors and the reduction potentials of the acceptors (eq 2, Table I). The redox parameters were all measured under identical conditions relative to ferrocene as a reference redox couple, using square-wave voltammetry at an ultramicro platinum disk electrode.<sup>8</sup> The decrease in  $k_{-e}$  with increasing reaction exothermicity is clearly illustrated in Figure 1. This effect is entirely analogous to the well-known example of radiationless transitions which become slower with increasing exothermicity (the energy gap law).<sup>9</sup> More importantly, the data

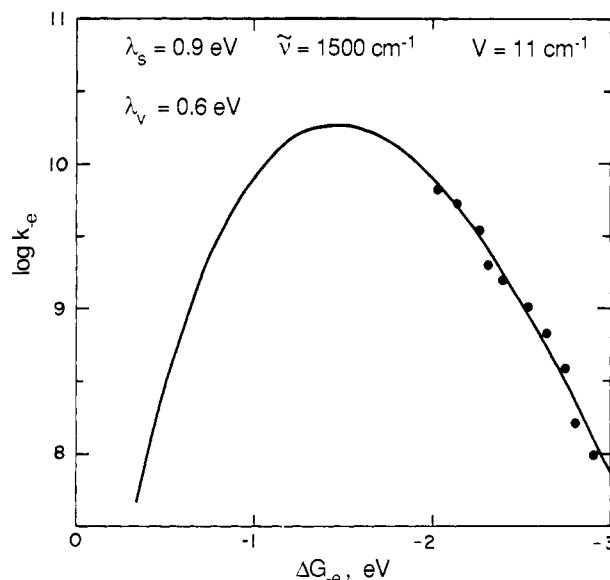


**Figure 1.** Log  $k_{-e}$  for return electron transfer within geminate ion pairs in acetonitrile at room temperature as a function of the free energy change for the reaction. The curve is calculated using eq 3 and the parameters shown in the figure. The maximum calculated rate is  $1.8 \times 10^{10} \text{ s}^{-1}$ .

provide a clear example of the Marcus inverted region in electron-transfer processes,<sup>4</sup> which obtained convincing experimental verification only recently.<sup>10</sup> The common feature of the electron-transfer processes in which the inverted region has been observed is that the reactions are first order and do not depend upon diffusive encounter of the donor and acceptor. The important conclusion to be drawn from the present results is that the inverted region also plays an extremely important role in bimolecular reactions in homogeneous solution at room temperature. The data can be described in terms of an accepted formulation of recent electron-transfer theories (eq 3, Figure 1).<sup>10a,11</sup> We follow Miller

$$k_{-e} = (\pi / \hbar^2 \lambda_s k_b T)^{1/2} |V|^2 \sum_{w=0}^{\infty} (e^{-S} S^w / w!) \exp\{-[(\lambda_s + \Delta G + w h \nu)^2 / 4 \lambda_s k_b T]\} \quad (3a)$$

$$S = \lambda_v / h \nu \quad (3b)$$

and Closs and assume that the important skeletal vibrations can be approximated by a single averaged mode ( $\nu$  in eq 3) of frequency of  $1500 \text{ cm}^{-1}$ , which is typical of carbon-carbon skeletal vibrations.<sup>10a,b</sup> The other parameters are  $S$ , which is the vibrational-electronic coupling strength (eq 3b);  $\lambda$ , the reorganizational energy which is divided into solvation ( $\lambda_s$ ) and vibration components ( $\lambda_v$ ); and  $V$ , the coupling matrix element. The three parameters  $\lambda_s$ ,  $\lambda_v$ , and  $V$  were adjusted in order to fit the calculated rate constants to the data (Figure 1). The range of  $\Delta G_{-e}$  is not sufficient to accurately define the values of the parameters, and other values within 0.2 V can also be found to fit the data.

Previously, Mataga et al. determined quantum yields for free-ion formation for various donor/acceptor pairs using flash photolysis.<sup>12</sup> However, in those studies either no correlation or very scattered correlations were observed between the kinetics and the ther-

(7) Weller, A. *Z. Phys. Chem. (Munich)* **1970**, *69*, 183.

(8) (a) Osteryoung, J. G.; Osteryoung, R. A. *Anal. Chem.* **1985**, *57*, 101A. (b) Whelan, D. P.; O'Dea, J. J.; Osteryoung, J. G. *J. Electroanal. Chem.* **1986**, *202*, 23.

(9) Siebrand, W. *J. Chem. Phys.* **1967**, *46*, 440.

(10) (a) Miller, J. R.; Beitz, J. V.; Huddleston, R. K. *J. Am. Chem. Soc.* **1984**, *106*, 5057. (b) Closs, G. L.; Calcaterra, L. T.; Green, N. J.; Penfield, K. W.; Miller, J. R. *J. Phys. Chem.* **1986**, *90*, 3673. (c) Wasielewski, M. R.; Niemczyk, M. P.; Svec, W. A.; Pewitt, E. B. *J. Am. Chem. Soc.* **1985**, *107*, 1080. (d) Irvine, M. P.; Harrison, R. J.; Beddard, G. S.; Leighton, P.; Sanders, J. K. M. *Chem. Phys.* **1986**, *104*, 315.

(11) (a) Van Duyne, R. P.; Fischer, S. F. *Chem. Phys.* **1974**, *5*, 183. (b) Ulstrup, J.; Jortner, J. *J. Chem. Phys.* **1975**, *63*, 4358. (c) Siders, P.; Marcus, R. A. *J. Am. Chem. Soc.* **1981**, *103*, 741, 748.

(12) (a) Shiomaya, H.; Masuhara, H.; Mataga, N. *Chem. Phys. Lett.* **1982**, *88*, 161. (b) Ohno, T.; Yoshimura, A.; Mataga, N. *J. Phys. Chem.* **1986**, *90*, 3295. (c) Mataga, N.; Kanda, Y.; Okada, T. *J. Phys. Chem.* **1986**, *90*, 3880.

modynamics of the return electron transfer. An excellent correlation is observed in the present work presumably because, unlike previous work, the compounds studied are similar in structure and dimensions and do not undergo significant chemical reactions either within or outside the geminate radical pair and because accurate redox parameters were obtained.

### Rhodium $\mu$ -Amido and $\mu$ -Imido A-Frame Complexes: Tautomeric Equilibria with a Deprotonated Bis(diphenylphosphino)methane Ligand<sup>1</sup>

Paul R. Sharp\* and Yuan-Wen Ge

Department of Chemistry  
University of Missouri—Columbia  
Columbia, Missouri 65211

Received February 27, 1987

Molecular A-frame complexes<sup>2</sup> are one of the larger classes of bimetallic late-transition-metal complexes. While a large number of apex ligands have been incorporated, apex oxo, imido, and amido ligands are unknown.<sup>3,4</sup> The majority of A-frame complexes are based on the bis(diphenylphosphino)methane (dppm) ligand and usually contain the metals Pt, Pd, Rh, or Ir.<sup>3,4a</sup> Since we are interested in preparing  $\mu$ -oxo and  $\mu$ -imido complexes of these metals as models for late-transition-metal surface oxides, we began working on expanding the A-frame class to include complexes with these apex ligands.<sup>1</sup> During this work we discovered the first examples of A-frame complexes containing a deprotonated dppm (bis(diphenylphosphino)methanide or dppm-H) ligand and at least two examples where the dppm ligand is involved in a unique tautomeric equilibrium. Although dppm-H ligands have been previously observed, the complexes have been monomers,<sup>5</sup> dimers with non-A-frame structures,<sup>6</sup> or clusters.<sup>7</sup> Our results show that the dppm-H ligand can support the A-frame structure. In addition, we have the first examples of A-frame complexes with bridging amido and imido ligands.

(1) Part 2 in a series entitled "Late-Transition-Metal  $\mu$ -Oxo and  $\mu$ -Imido Complexes". For part 1, see: Sharp, P. R.; Flynn, J. R. *Inorg. Chem.*, in press.

(2) Kubiak, C. P.; Eisenberg, R. *J. Am. Chem. Soc.* **1977**, *99*, 6129-6131; *Inorg. Chem.* **1980**, *19*, 2726-2732.

(3) Puddephatt, R. *J. Chem. Soc. Rev.* **1983**, *12*, 99-128.

(4) (a) Balch, A. L. In *Catalytic Aspects of Metal Phosphine Complexes*; Alyea, E. C., Meek, D. W., Ed.; American Chemical Society: Washington, DC, 1982; *Adv. Chem. Ser.* **1982**, *No. 196*, 243-255. (b) Jandik, P.; Schubert, U.; Schmidbaur, H. *Angew. Chem., Int. Ed. Engl.* **1982**, *21*, 72; *Angew. Chem. Suppl.* **1982**, 1-12. (c) Murray, H. H.; Fackler, J. P., Jr.; Mazany, A. M. *Organometallics* **1984**, *3*, 1310-1311. Knachel, H. C.; Dudis, D. S.; Fackler, J. P., Jr. *Ibid.* **1985**, *4*, 154-157.

(5) (a) Bassett, J.-M.; Mandl, J. R.; Schmidbaur, H. *Chem. Ber.* **1980**, *113*, 1145-1152. (b) Browning, J.; Bushnell, G. W.; Dixon, K. R. *J. Organomet. Chem.* **1980**, *198*, C11. (c) Brown, M. B.; Yavari, A.; Manojlovic-Muir, L.; Muir, K. W.; Moulding, R. J.; Seddon, K. R. *J. Organomet. Chem.* **1982**, *236*, C33-C36. (d) Al Jibori, S.; Shaw, B. L. *Inorg. Chim. Acta* **1983**, *74*, 235-239.

(6) (a) Dawkins, G. M.; Green, M.; Jeffery, J. C.; Stone, F. G. A. *J. Chem. Soc., Chem. Commun.* **1980**, 1120. (b) Briant, C. E.; Hall, K. P.; Mingsos, D. M. P. *J. Organomet. Chem.* **1982**, *229*, C5-C8. (c) Brown, M. B.; Yavari, A.; Manojlovic-Muir, L.; Muir, K. W. *J. Organomet. Chem.* **1983**, *256*, C19-C22.

(7) (a) Camus, A.; Marsich, N.; Nardin, G.; Randaccio, L. *J. Organomet. Chem.* **1973**, *60*, C39-C42. (b) van der Velden, J. W. A.; Bour, J. J.; Vollenbrock, F. A.; Beurskens, P. T.; Smits, J. M. M. *J. Chem. Soc., Chem. Commun.* **1979**, 1162-1163. (c) Uson, R.; Laguna, A.; Laguna, M.; Gemeno, M. C.; Jones, P. G.; Fittschen, C.; Sheldrick, G. M. *J. Chem. Soc., Chem. Commun.* **1986**, 506-510.

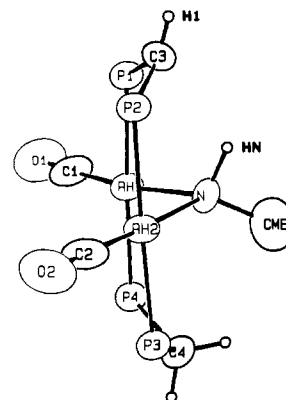
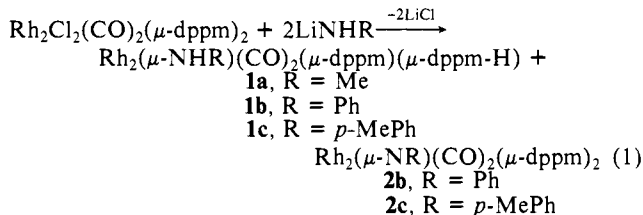


**Figure 1.** ORTEP view of  $\text{Rh}_2(\mu\text{-NHMe})(\text{CO})_2(\mu\text{-dppm})(\mu\text{-dppm-H})$  (**1a**) 50% probability ellipsoids. Phenyl rings are omitted for clarity. Selected distances (Å) and angles (deg): P1-C3, 1.738 (8); P2-C3, 1.736 (8); P3-C4, 1.837 (7); P4-C4, 1.851 (7); C3-H1, 0.80 (9); Rh1-N, 2.107 (6); Rh2-N, 2.091 (5); N-HN, 1.09 (9); HN-C3, 2.23; P1-C3-P2, 119.3 (4); P1-C3-H1, 119 (7); P2-C3-H1, 115 (7); Rh1-N-Rh2, 94.4 (2); Rh-N-CME, 121.0 (5); Rh2-N-CME, 127.5 (5); Rh1-N-HN, 116 (4); Rh2-N-HN, 103 (4); CME-N-HN, 96 (4); N-HN-C3, 128 (4).

Treating yellow  $\text{Rh}_2\text{Cl}_2(\text{CO})_2(\mu\text{-dppm})_2$ <sup>8</sup> with 2 equiv of LiNHR in ether gives a single orange product (**1a**) when R = Me (eq 1). Spectroscopic<sup>9</sup> and X-ray<sup>11</sup> data show **1a** to be a



$\mu$ -methylamido A-frame complex with a dppm-H ligand. A view of the molecular structure is shown in Figure 1.

When R = Ph or *p*-MePh a mixture of two products (eq 1, **1b** and **2b** for R = Ph, **1c** and **2c** for R = *p*-MePh) is obtained as shown by IR.<sup>12</sup> Experiments on the slower NMR time scale show that the two products are in rapid equilibrium, a slow exchange

(8) Prepared by a modified procedure of: Mague, J. T. *Inorg. Chem.* **1969**, *8*, 1975. Mague, J. T.; Mitchener, J. P. *Ibid.* **1969**, *8*, 119 as given in ref 2.

(9) Data for **1a**. Anal. Calcd (found) for  $\text{Rh}_2\text{P}_4\text{NO}_2\text{C}_3\text{H}_5$ : C, 60.07 (59.60); H, 4.47 (4.50); N, 1.32 (1.08). IR ( $\text{cm}^{-1}$ ) ( $\text{CH}_2\text{Cl}_2$ ) 1965 s and 1949 vs ( $\nu_{\text{CO}}$ ); (mineral oil) 3137 w ( $\nu_{\text{NH}}$ ). <sup>1</sup>H NMR (300 MHz,  $\text{C}_6\text{D}_6$ , 22 °C)  $\delta$  6.8-8.2 (m, 40, Ph), 3.58 and 3.24 (m, 2,  $\text{CH}_2$ ), 3.39 (br m, 1, NH), 2.23 (m, 3, NCH<sub>3</sub>), 1.61 (br m, 1, CH). Assignments were confirmed by <sup>13</sup>C/<sup>1</sup>H shift correlation experiments. The NCH<sub>3</sub> peak sharpened and increased in intensity when the NH peak was irradiated. <sup>13</sup>C NMR (75 MHz,  $\text{CD}_2\text{Cl}_2$ , 10 °C)  $\delta$  193.7 (m, CO), 135-127 (Ph), 43.5 (s, NCH<sub>3</sub>), 31.4 (t,  $J_{\text{CP}}$  = 10.1 Hz, PCH<sub>2</sub>P), 9.1 (t,  $J_{\text{CP}}$  = 53.0 Hz, PCHP). Assignments were confirmed by DEPTH<sup>10</sup> experiments. <sup>31</sup>P NMR (121 MHz,  $\text{CH}_2\text{Cl}_2/\text{C}_6\text{D}_6$ , external  $\text{H}_3\text{PO}_4$  reference, 22 °C), symmetric AA'BB'XX' pattern centered at 24 ppm spanning 18-30 ppm. Approximately simulated with the following parameters:  $J_{\text{AA}'} = J_{\text{BB}'} = 30$  Hz;  $J_{\text{AB}} = J_{\text{A'B'}} = 300$  Hz;  $J_{\text{AB}'} = J_{\text{A'B}}$  = 12 Hz;  $J_{\text{AX}} = J_{\text{BX}} = J_{\text{A'X}'} = J_{\text{B'X}'} = 80$  Hz;  $J_{\text{AX}'} = J_{\text{BX}'} = J_{\text{A'X}} = J_{\text{B'X}}$  = 12 Hz;  $J_{\text{XX}'} = 0$  Hz;  $\delta(\text{A}) = \delta(\text{A}')$  = 20 ppm; and  $\delta(\text{B}) = \delta(\text{B}')$  = 28 ppm.

(10) Daddrell, D. M.; Pegg, D. J.; Bendell, M. R. *J. Magn. Reson.* **1982**, *48*, 323-327.

(11) Crystals from toluene:  $\text{Rh}_2\text{P}_4\text{O}_2\text{NC}_3\text{H}_5\text{H}_7\text{-C}_7\text{H}_5$ , fw = 1151.82,  $d_{\text{calcd}} = 1.30$ , triclinic ( $P\bar{1}$ ),  $a = 10.459$  (12) Å,  $b = 14.348$  (3) Å,  $c = 20.867$  (6) Å,  $\alpha = 104.96$  (2)°,  $\beta = 101.12$  (4)°,  $\gamma = 93.47$  (6)°,  $V = 2948.3$  Å<sup>3</sup>, and  $Z = 2$ . Full-matrix least-squares calculations converged to  $R(F_o) = 0.050$  and  $R_w(F_o) = 0.081$  for 4075 observations above  $2\sigma$ . Positions for H1 and HN (see Figure 1) were refined. Full structural details will be reported in a forthcoming publication.

(12) **1b/2b** (R = Ph). IR ( $\text{cm}^{-1}$ ) ( $\text{CH}_2\text{Cl}_2$ ) 1964 w, 1942 br s, 1929 vs ( $\nu_{\text{CO}}$ );  $\nu_{\text{NH}}$  for **1b** was not observed (mineral oil). <sup>31</sup>P NMR (121 MHz,  $\text{CH}_2\text{Cl}_2/\text{C}_6\text{D}_6$  (2:1), external  $\text{H}_3\text{PO}_4$  reference, 22 °C)  $\delta$  23.2 (d,  $J_{\text{RHP}} = 145$  Hz). **1c/2c** (R = *p*-MePh). IR ( $\text{cm}^{-1}$ ) ( $\text{CH}_2\text{Cl}_2$ ) 1964 m, 1945 vs, 1927 m ( $\nu_{\text{CO}}$ ); (mineral oil) 3138 w ( $\nu_{\text{NH}}$ ). <sup>31</sup>P NMR (121 MHz,  $\text{CH}_2\text{Cl}_2/\text{C}_6\text{D}_6$  (2:1), external  $\text{H}_3\text{PO}_4$  reference, 22 °C)  $\delta$  22.6 (br d,  $J_{\text{RHP}} = 138$  Hz). At -80 °C this peak was resolved into a doublet at 21.9 ppm ( $J_{\text{RHP}} = 136$  Hz) for **2c** and a symmetric AA'BB'XX' pattern for **1c** centered at 21 ppm and spanning 13-30 ppm ( $T_c = -68$  °C). Approximate ratio of **1c** to **2c** at -80 °C was 2:3. Assuming an equal population at  $T_c$ ,  $\Delta G^\ddagger \sim 40$  kJ/mol.